Journal of
Marine Science and Engineering

MDPI

Article

Effect of Tip Clearance on Force Characteristics of Helical Axial-Flow Blade Pumps under Cavitation Conditions

Haigang Wen [1,2,*], Luyao Li [1,2], Guangtai Shi [1,2], Haijun Ma [3] and Xiaodong Peng [1,2]

1 Key Laboratory of Fluid and Power Machinery, Xihua University, Ministry of Education, Chengdu 610039, China; sgtaixh@126.com (G.S.)
2 Key Laboratory of Fluid Machinery and Engineering, Xihua University, Chengdu 610039, China
3 Sichuan Chuantou Tianwan Hydropower Development Co., Ltd., Chengdu 610000, China
* Correspondence: whg@mail.xhu.edu.cn

Abstract: A spiral axial-flow blade pump (SABP), as the core piece of equipment in the oil and natural gas closed-gathering and transportation process, can not only transport gas–liquid mixtures with a high gas content, but can also transport gas–liquid–solid mixtures containing small amounts of sand. However, due to the complexity of the distribution of transport media groups and the uncertainty of internal flow processes, large vortices often appear in the passage of the pumps, and the existence of vortices can easily induce the occurrence of pump cavitations. In the present work, a self-developed SABP was taken as the research object, and the cavitation performance of the SABP was numerically calculated. The pressure load variation under different tip clearances and different cavitation stages was analyzed, and the characteristics of the axial and radial forces were also analyzed in detail.

Keywords: spiral axial-flow blade pump; numerical calculation; cavitation performance; tip clearance; force characteristic

Citation: Wen, H.; Li, L.; Shi, G.; Ma, H.; Peng, X. Effect of Tip Clearance on Force Characteristics of Helical Axial-Flow Blade Pumps under Cavitation Conditions. *J. Mar. Sci. Eng.* **2023**, *11*, 2299. https://doi.org/10.3390/jmse11122299

Academic Editor: Atilla Incecik

Received: 9 November 2023
Revised: 25 November 2023
Accepted: 28 November 2023
Published: 4 December 2023

1. Introduction

Because of their dual characteristics of acting as a pump and a compressor, SABPs can achieve mixed oil-and-gas transportation under complex working conditions, but their transportation performance is affected by many aspects, such as the gas content and tip-leakage loss. Tip-leakage dissipation mainly refers to the energy loss induced by tip-clearance-leakage vortex cavitation during pump operations. Due to the leakage flow and cavitation, the flow characteristics are very complicated. Therefore, the effect of cavitation evolution under different tip-clearance sizes is a highlighted area of research.

At present, some scholars have conducted research on SABPs. Deepak Meerakaviyad et al. [1] reviewed the latest research advances in spiral blade pumps and used a computational fluid dynamics (CFD) method to predict the flow behaviors of fluid mixtures. Hao et al. [2] used a genetic algorithm to optimize a spiral blade pump, and the efficiency of the pump was increased by 1.91%. Kim et al. [3] adopted an experimental design method and found that the optimized model had less energy dissipation than the basic model. Yang et al. [4,5] studied the characteristics of multiphase pumps with a high gas content by developing a comprehensive synchronal rotary multiphase (SRMP) model and found that, under a given pressure difference, the leakage dissipation increased significantly with an increase in the gas content. As a result, the volume flow of the SRMP was significantly reduced. Liu et al. [6,7] analyzed the effects of viscosity, flow rate, and blade height on the turbulent kinetic energy, revealed the impacts of viscosity by using partial differential equations, established a theoretical model for predicting flow effects, and proposed a method for optimizing multistage mixed-transport pumps based on an Oseen vortex theory prediction.

Cavitation not only occurs in the impeller passage of fluid machinery, but also in the impeller blade tip clearance, which results in an obvious adverse effect on the operation of fluid machinery. At the same time, it is accompanied with the occurrence of unstable flow conditions, such as TLVs, tip-clearance secondary-leakage vortices, and tip-clearance separation vortices. Therefore, it is very important to study cavitation in the tip clearance of a fluid machine. Shen et al. [8,9] investigated the cavitation characteristics of TLVs in an axial-flow pump using experimental and numerical methods, clarified the effect of tip-clearance cavitation on the flow in the pump, and further revealed the pump's internal mechanism. Zhao et al. [10] investigated the influence of tip clearance on the cavitation performance of axial-flow pumps, and the results showed that the cavitation degree at the impeller rim increased with an increase in the tip clearance. Zhang et al. [11] explored the evolution mechanism of TLVs and analyzed the influence of the tip-clearance width; they found that the leakage shear zone is the main region for the formation of tip-leakage vortices and the distribution of vortices and cavitation is basically the same under a large cavitation number. Zhang et al. [12,13] studied TLVs and their cavitation characteristics in an axial-flow pump and proposed that the SST k-ω turbulence model has good applicability in the calculation. Li et al. [14] conducted similar research and found that the TLV intensity gradually increased and the critical cavitation number gradually decreased with the growth of tip clearance under low-flow-rate cases. Moreover, TLVs resulted in secondary flow, vortices, and other flow-instability phenomena [15]. Han et al. [16] numerically calculated the flow characteristics in a water-jet propulsion pump and revealed that the axial velocity at the impeller outlet reduces faster with the growth of tip-clearance size. Shi et al. [17] took the numerical technology and an experimental method to investigate the full-channel scale model pump of the South-to-North Water Diversion project and found that, as the tip clearance increased, the critical cavitation number of the model pump also increased. Zhang et al. [18] revealed the evolution mechanism and vortex cavitation in axial-flow pumps and proposed that the leakage shear zone is the main area where the leakage flow enters the suction surface to form TLVs. Han et al. [19] used the large eddy simulation method and the ZGB cavitation model to numerically calculate the cavitation flow and found that the development of cavitation intensified the generation of vorticity near the blade tip and promoted flow instability. Xu et al. [20] investigated the tip-leakage cavitation flow with NACA0009 hydrofoil using a new cavitation model combined with LES and discovered that the stretching term was dominant, regardless of the tip-leakage size. Shamsuddeen et al. [21] focused their research on the tip-clearance cavitation of axial-flow propeller turbines occurring between the blade tip and the fixed envelope shell and studied the cavitation mitigation function generated by anti-cavitation fins. Xu et al. [22] also explored the characteristics of TLVs and different tip-clearance sizes in axial-flow pumps. Fanning et al. [23] simulated the return flow in the inducer under different tip-clearance sizes and found that the clearance leakage flow was eliminated without tip clearance, but the return flow could still be observed.

To sum up, many scholars have conducted extensive and in-depth research on the cavitation of fluid machinery. Since the impeller rotation needs to consider the influence of the blade-tip-clearance size on the flow in the entire flow channel, research on tip-clearance cavitation flow can result in a better grasp of the flow mechanism of the flow field in a pump. Therefore, it is particularly important to analyze the cavitation performance of tip clearance in the impeller region of helical blade pumps. Combined with experimental verification, this paper mainly adopts a numerical calculation method to study the cavitation flow near the blade-tip-clearance region of a helical blade pump. The pressure load variation in the tip clearance, with different dimensions in different cavitation stages, was analyzed, and the impact of tip clearance on the axial and radial forces under cavitation conditions was analyzed in detail.

2. Computational Model and Numerical Method

2.1. Numerical Simulation Theory

(1) Volume fraction and momentum equation of gas–liquid two-phase flow

The volume fraction and momentum equation of liquid vapor two-phase cavitating flows in the pipeline are:

$$\frac{\partial \alpha_v}{\partial t} + \frac{\partial(\alpha_v u_i)}{\partial x_i} = 0 \tag{1}$$

$$\frac{\partial u_i}{\partial t} + \frac{\partial(u_i u_j)}{\partial x_j} = \frac{1}{\rho_m}\left\{-\frac{\partial p}{\partial x_i} + \frac{\partial}{\partial x_j}\left[\mu_m\left(\frac{\partial u_i}{\partial x_j} + \frac{\partial u_j}{\partial x_i}\right)\right] - F_{sfi}\right\} + f_i \tag{2}$$

$$\alpha_w + \alpha_v = 1 \tag{3}$$

where $u_{\mathbf{i}}$ and p denote the velocity and the pressure of the vapor–water mixture, respectively; α_{v} and α_{w} are the volume fraction of vapor and water, respectively; f_{i} is the body force considering the gravitational acceleration; τ_{ij} is the shear stress of the mixture; F_{sfi} is the surface tension force; $\rho_{\mathbf{m}}$ and $\mu_{\mathbf{m}}$ are the density and the dynamic viscosity of the mixture, respectively, and are dependent on the vapor volume fraction, as follows:

$$\rho_{\mathrm{m}} = \alpha_{\mathrm{v}}\rho_{\mathrm{v}} + (1-\alpha_{\mathrm{v}})\rho_{\mathrm{w}} \tag{4}$$

$$\mu_{\mathrm{m}} = \alpha_{\mathrm{v}}\mu_{\mathrm{v}} + (1-\alpha_{\mathrm{v}})\mu_{\mathrm{w}} \tag{5}$$

where ρ_{w} is the density of water; $\mu_{\mathbf{w}}$ and $\mu_{\mathbf{v}}$ are the dynamic viscosities of water and vapor, respectively.

(2) ZGB Cavitation Model

The ZGB cavitation model can accurately simulate the quasi-periodicity cavitation phenomenon and its evolution process. The interphase transmission rate is described as below:

When P_{v} is less than P:

$$R_{\mathrm{c}} = F_{\mathrm{cond}}\frac{3\alpha_{\mathrm{v}}\rho_{\mathrm{v}}}{R_B}\sqrt{\frac{2}{3}\frac{P-P_{\mathrm{v}}}{\rho_1}} \tag{6}$$

When P is less than P_{v}:

$$R_{\mathrm{e}} = F_{\mathrm{vap}}\frac{3\alpha_{\mathrm{nuc}}(1-\alpha_{\mathrm{v}})\rho_{\mathrm{v}}}{R_B}\sqrt{\frac{2}{3}\frac{P_{\mathrm{v}}-P}{\rho_1}} \tag{7}$$

(3) Turbulence Model

The SST k-ω turbulence model is expressed as follows:

$$\rho\frac{\partial k}{\partial t} + \frac{\partial(\rho v_i k)}{\partial x_i} = \frac{\partial}{\partial x_j}\left[\left(v + \frac{v_i}{\sigma_k}\right)\frac{\partial k}{\partial x_j}\right] + G_k - \beta\rho k\omega \tag{8}$$

$$\frac{\partial}{\partial t}(\rho\omega) + \frac{\partial}{\partial x_j}(\rho v_j\omega) = \frac{\partial}{\partial x_j}\left[\left(\mu + \frac{\mu_t}{\sigma_\omega}\right)\frac{\partial\omega}{\partial x_j}\right] + G_\omega - \rho\beta\omega^2 + D_\omega \tag{9}$$

2.2. Computational Model

A booster unit (first stage impeller and diffuser) of the SABP was selected as the calculation model. To prevent interference with the simulation, the import and export extension sections were extended appropriately. To investigate the effect of different tip clearance on the cavitation performance of the SABP, three schemes with tip clearance Rtc sizes of 0.5, 1.0 and 1.5 mm were adopted. The design parameters and models are illustrated in Table 1 and Figure 1.

Table 1. Design parameters of the SABP.

Parameters	Value	Unit
Flowrate Q	100	m^3/h
Speed n	3600	rpm
Impeller blade numbers	3	-
Diffuser blade numbers	11	-

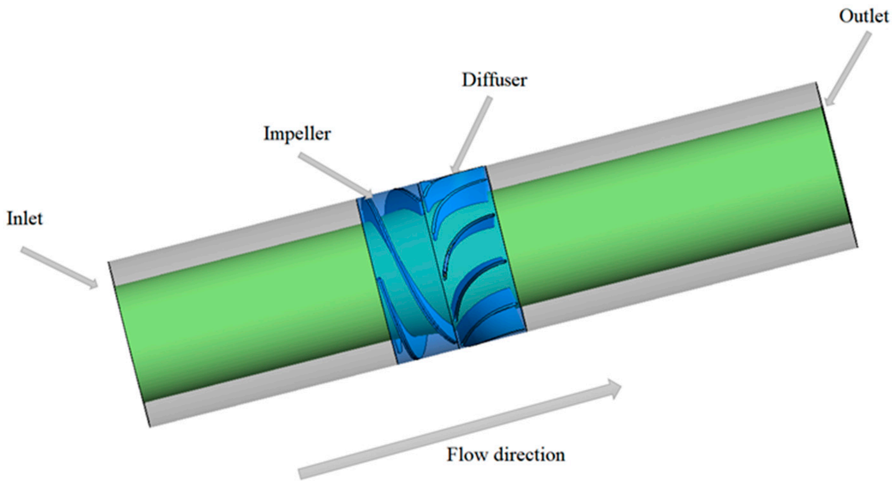

Figure 1. Calculation model.

2.3. Mesh and Independent Verification

A single blade was intercepted by Ansys Geometry to divide the impeller or diffuser channel. Then, the geometric structure of the divided flow channel was imported into Ansys TurboGrid for structural hexahedral mesh. Ansys ICEM was adopted to divide the structural hexahedral mesh of the inlet extension and the outlet extension of the ASBP. Finally, in Ansys CFX software, a single impeller and a diffuser were assembled by removing their interface.

To satisfy the calculation accuracy and accurate simulation of tip clearance flow field, 30 layers of mesh were used to encrypt the impeller domain mesh, and 20 layers of mesh spacing remained unchanged. Five schemes of mesh were selected to verify mesh independence, and the results are shown in Table 2. With the growth in the mesh numbers, the variation in heads between scheme 3, scheme 4 and scheme 5 tended to be stable, meeting the requirements of simulation accuracy. Considering the comprehensive consideration of factors such as time cost, calculation cycle and calculation reliability, mesh scheme 3 was finally selected. It also met the requirements of mesh independence, and the mesh division results were illustrated in Figure 2.

Table 2. Mesh independence verification.

Mesh Scheme	Mesh Number	Head/m
1	2,167,300	13.93
2	2,496,556	13.79
3	3,251,714	13.56
4	3,958,986	13.57
5	6,078,160	13.58

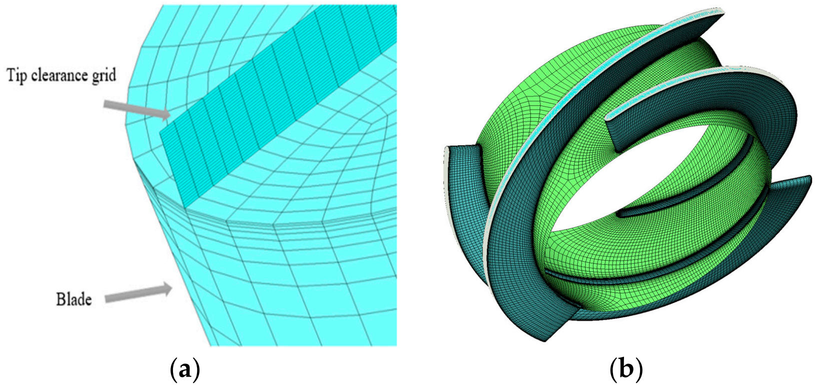

Figure 2. Mesh generation: (**a**) local impeller mesh; (**b**) impeller mesh.

2.4. Boundary Condition

Firstly, the steady calculation with the non-cavitation model was carried out with the single-phase pure water, and the calculation result was taken as the initial value. Then, the flow field was calculated twice, after obtaining the stable steady calculation result. Finally, the unsteady calculation was carried out and stopped when the convergence condition was reached.

The ASBP inlet boundary condition was set as the pressure, and the export condition was the quality. Inlet liquid phase volume fraction and vapor phase volume fraction were set to 1 and 0, respectively. The wall function adopted a non-slip wall, and the impeller rotating angular speed was 3000 r/min. The interface surface between the inlet extension section and the impeller and the interface surface between the impeller and the diffuser were set as the frozen rotor, and the matching angle was adopted, and the supporting parts on both sides were set at 360 degrees. Since the study of the SABP cavitation performance needs to compare the flow field changes in different cavitation cases, reducing the inlet pressure was adopted to realize the calculation of cavitation conditions in different stages.

3. Experimental Rig and Numerical Verification

3.1. Experimental Rig

The SABP test bench was designed and built, and the results of external characteristic testing of the SABP were used to verify the reliability of the numerical calculation results. The SABP booster unit is shown in Figure 3 and the SABP experimental system is shown in Figure 4. Figure 5 shows the schematic diagram of the test system.

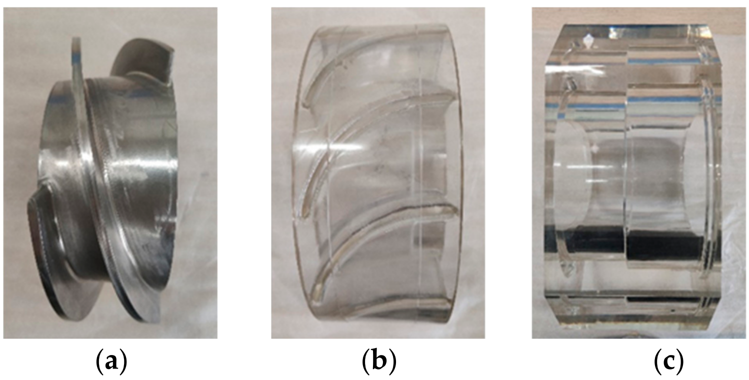

Figure 3. SABP booster unit: (**a**) impeller; (**b**) diffuser; (**c**) pump body.

Figure 4. SABP test system.

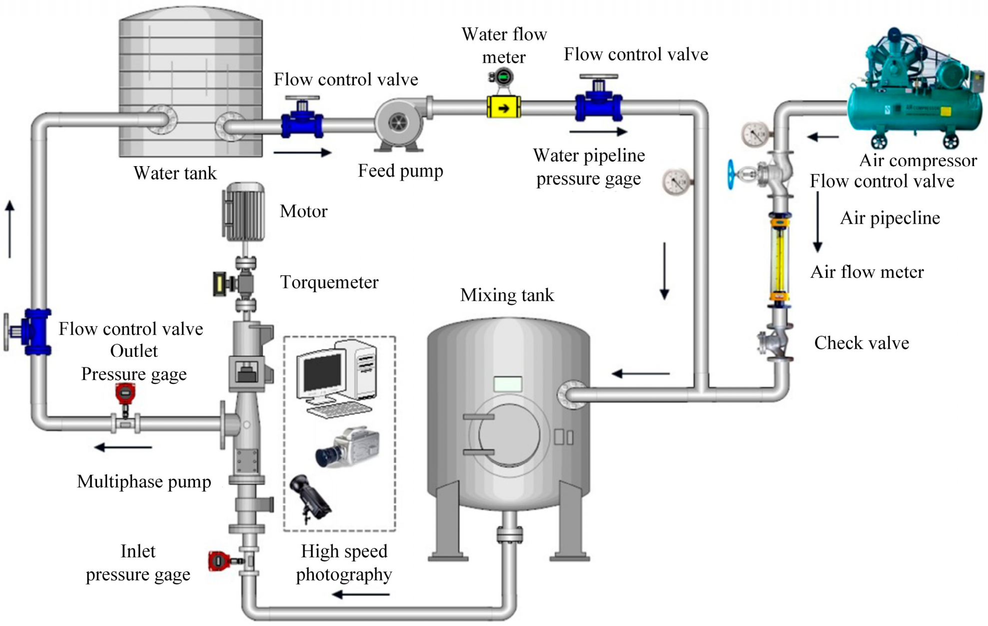

Figure 5. Schematic diagram of SABP test system.

3.2. Numerical Verification

The test results and numerical calculation results were drawn into the external characteristic curve, as shown in Figure 6. The relative error of head and efficiency and the numerical calculation results is less than 5%, which indicates the reliability of the numerical calculation results.

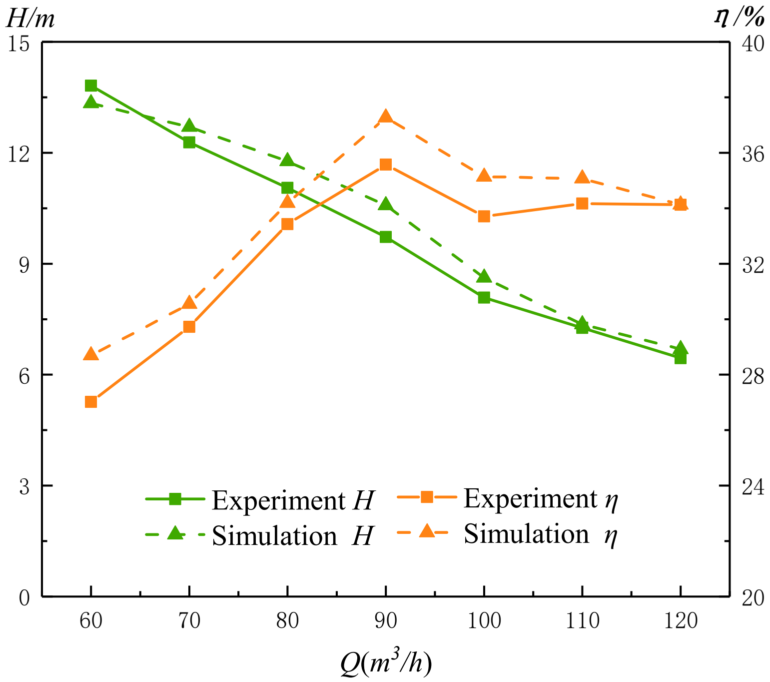

Figure 6. External characteristic curve of numerical and experimental results.

4. Results and Discussion

With the decrease in cavitation numbers, the head of the SABP also reduces gradually. When the head reduces by 3%, the cavitation reaches the critical cavitation point. When the head reduces by 7%, the cavitation reaches the severe cavitation point. When the head drops by 20%, fracture cavitation occurs. In this article, the cavitation characteristics of the SABP were studied under the above three defined cavitation stages.

4.1. Effect of Cavitation Number on Head of the Pump under Different Tip Clearances

Figure 7 shows the head variation curve of the SABP. When Rtc = 0.5 mm, the pump head reaches 13.63 m without cavitation. When the critical cavitation point reaches the cavitation number of 0.52, the stage of severe cavitation reaches the cavitation number of 0.29, and the fracture cavitation point reaches the cavitation number of 0.2.

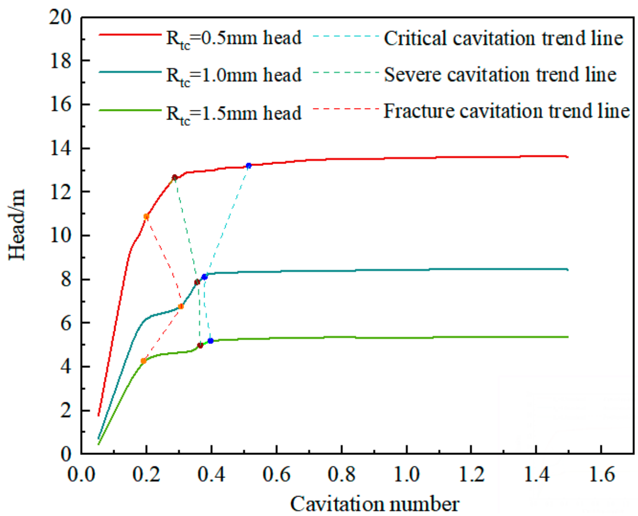

Figure 7. Cavitation characteristic curves under different tip clearance sizes.

When Rtc = 1.0 mm, the pump head without cavitation decreases with the cavitation number and reaches the critical cavitation point at the cavitation number of 0.38, develops to the serious cavitation stage at the cavitation number of 0.36, and reaches the fracture cavitation point at the cavitation number of 0.31.

When Rtc = 1.5 mm, the pump head reaches 5.36 m without cavitation. The critical cavitation point reaches the cavitation number of 0.4, the stage of severe cavitation reaches the cavitation number of 0.37, and the fracture cavitation point reaches the cavitation number of 0.19. The above data show that the tip clearance size and cavitation number have significant effects on the head of the SABP.

4.2. Effect of Tip Clearance Sizes on Pressure Load Distribution of the Impeller Surface

In this article, flow direction is defined as follows: along the direction of the impeller or the diffuser's blade profile, the position of the blade inlet is dimensionless to the position of the blade outlet, the inlet position is 0, and the outlet position is 1.

From Figure 8, it can be seen that at the critical cavitation stage, tip clearance has a noticeable impact on the pressure load in the flow direction of 0.1 to 1.0. In the flow direction of 0 to 0.1 and 0.9 to 1.0, there are sudden changes in the pressure load, mainly caused by dynamic and static interference. The pressure of both the blade PS (pressure surface) and SS (suction surface) reduces with the growth in tip clearance, and only the pressure on the blade PS reduces with the growth in tip clearance along the flow direction from 0.4 to 1.0. In the severe cavitation case, the tip clearance is equal to 0.5 mm, the pressure on the PS and the SS along the flow direction decreases significantly, and other changes are the same as those in the critical cavitation case. In the fracture cavitation case, and the tip clearance is equal to 0.5 mm, the pressure on the PS and the SS along the flow direction obviously reduces again. Under the case where the tip clearance is equal to 1.5 mm, the pressure on the PS and the SS also reduces along the flow direction, and the pressure on the SS drops to 0 at the flow direction from 0.5 to 0.9. Tip clearance impacts the entire impeller passage in different cavitation cases, but the influence on 1.0 mm tip clearance is the least. The development of cavitation further intensifies the reduction in blade surface pressure.

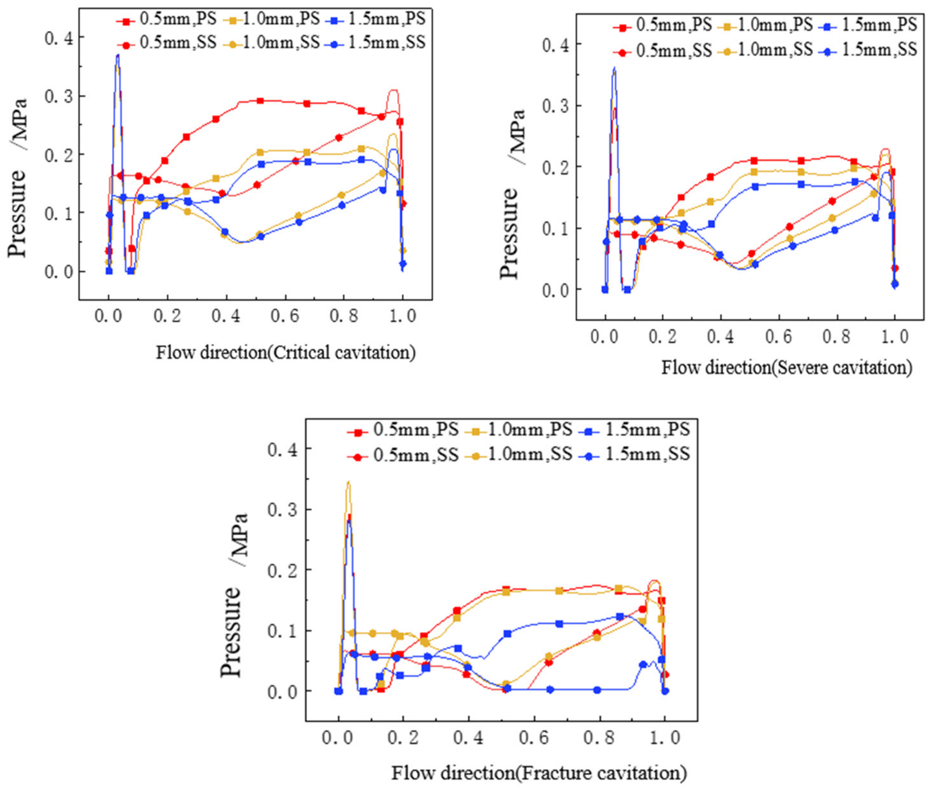

Figure 8. Pressure load in the impeller of the SABP at different tip clearance sizes.

4.3. Influence of Tip Clearance of Different Dimensions on Pressure Load Distribution of the Diffuser Surface

Figure 9 shows the pressure load distribution on the SS and the PS in the diffuser region. From Figure 9, in the critical cavitation case, tip clearance has a noticeable influence on the pressure load, and sudden changes in the pressure load also occur in the flow direction from 0 to 0.1, and the blade surface pressure in the entire flow section reduces with the growth in tip clearance size. The blade surface pressure with a tip clearance of 0.5 mm is obviously higher than that under other cases. In the severe cavitation stage, the pressure of the 0.5 mm tip clearance obviously reduces, but the pressure in the 0.1 to 0.9 section of the flow direction still reduces with the growth in tip clearance. In the fracture cavitation case, the pressure from the diffuser inlet to the outlet section reduces significantly under all tip clearance conditions, and the pressure difference between 1.0 mm tip clearance and 0.5 mm tip clearance conditions shrinks significantly. The pressure load curve distribution between the two tip clearance conditions is very close, and the difference in the pressure load at the tip clearance of 1.5 mm is significantly increased. The pressure under tip clearance is affected differently in different cavitation stages.

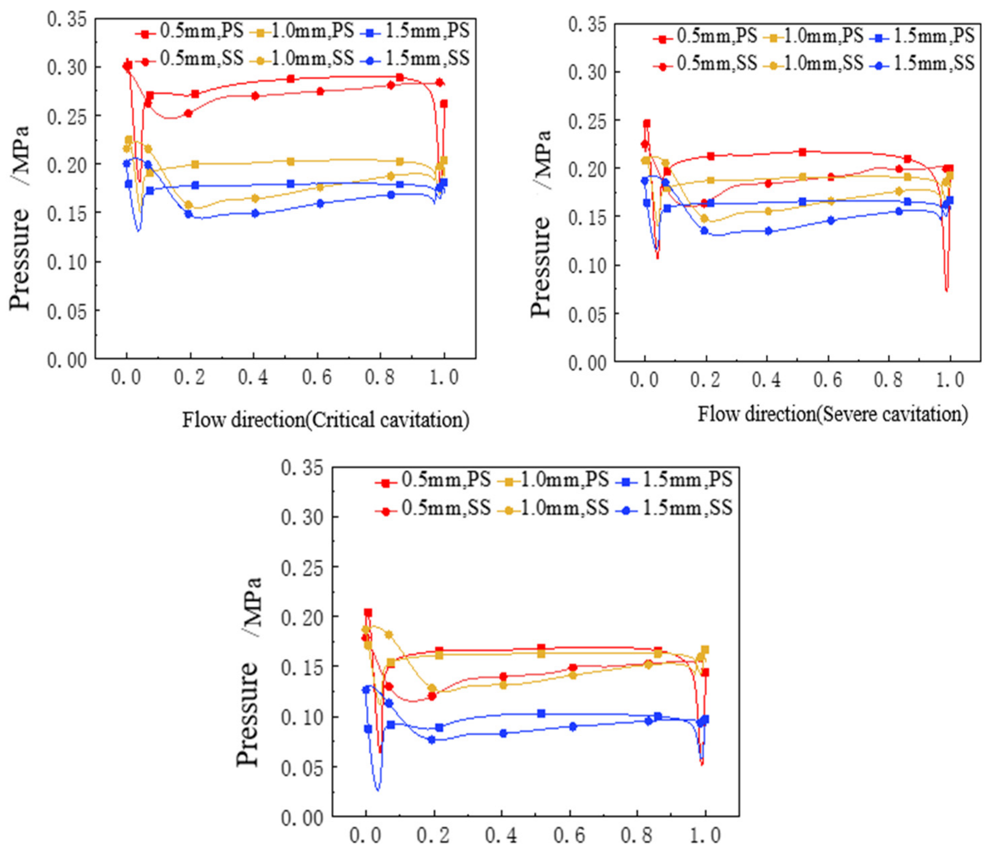

Figure 9. Pressure load distribution in the diffuser region of the SABP under different tip clearance sizes.

4.4. Effect of Tip Clearance on Axial and Radial Forces of the Impeller

Figure 10 displays the axial force distribution in the impeller.

Figure 10 shows the axial force changes from the impeller inlet to the impeller in different cavitation cases. In the critical cavitation case, the tip clearance impacts the axial force along the entire flow direction of the impeller, and the effect on the back of the impeller is the most obvious. The axial force declines when the growth in tip clearance first presents a decreasing trend, then displays an increasing trend along the flow direction. When the tip clearance is 0.5 mm and 1.0 mm, the axial force reaches the minimum value in the flow direction of 0.2 section, and the tip clearance is equal to 1.5 mm, the axial force reaches the minimum value in the flow direction of 0.3 section. In the severe cavitation stage, the effect of tip clearance size on axial force is roughly the same as that in the critical cavitation stage. The main change is that when the tip clearance is 0.5 mm, the axial force along the flow direction reduces significantly. In the fracture cavitation stage, the axial force along the flow direction reduces further at the tip clearance of 0.5 mm, and the axial force along the flow direction also reduces to a certain extent at the tip clearance of 1.5 mm. The other changes are the same as in the previous two cavitation stages.

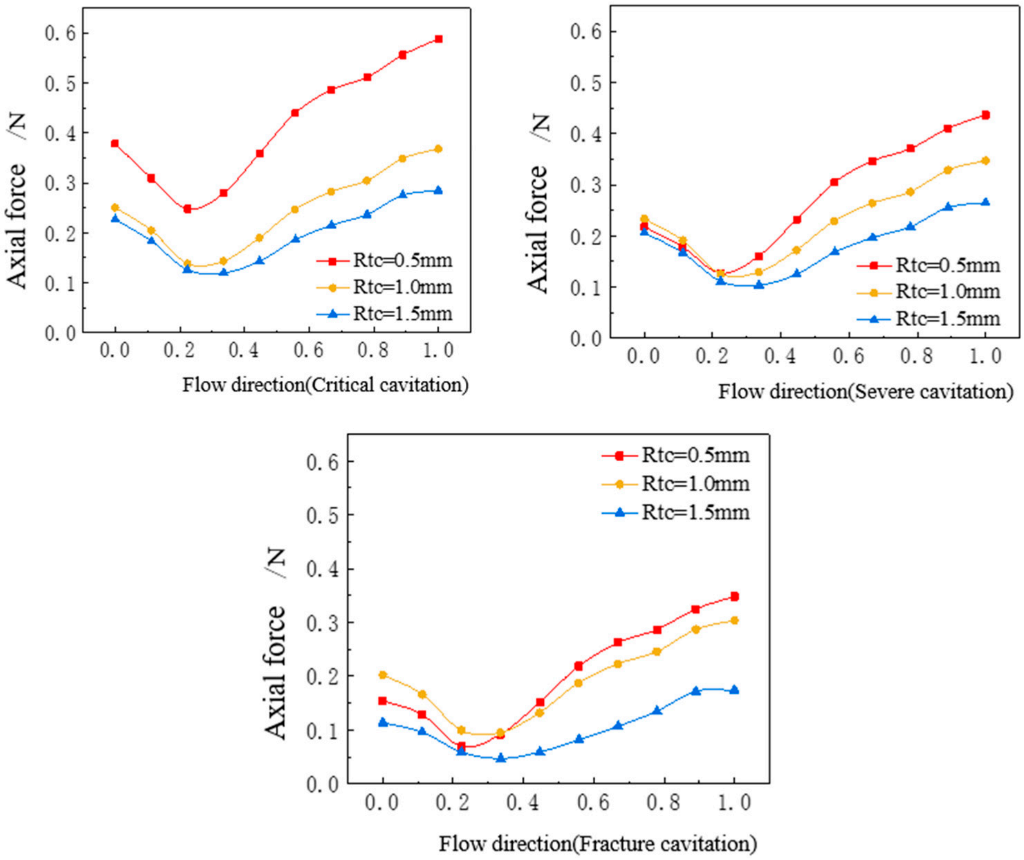

Figure 10. Axial force in the impeller of the SABP at different tip clearance sizes.

From Figure 11, the regulation of radial force from the impeller inlet to the impeller is the same. In the critical cavitation case, tip clearance has different degrees effect on the radial force of the impeller, and the influence is greatest in its front section. The radial force reduces with the growth in tip clearance size along the flow direction from 0 to 0.6, and increases with the growth in tip clearance size along the flow direction from 0.6 to 0.8. In the severe cavitation stage, the effect of tip clearance on radial force is the same as that in the critical cavitation case. In the fracture cavitation case, when the tip clearance is 0.5 mm and 1.0 mm, the radial force reduces in the flow direction from 0.2 to 0.3. The radial force change at the tip clearance of 1.0 mm is the same as that at the tip clearance of 1.5 mm case. In the tip clearance of the 1.5 mm case, the radial force increases in the flow direction of 0.4 to 0.5 mm, and at the tip clearance of 0.5 mm case along the flow direction from 0.9 to 1.0, the radial force increases, and the change trend is the same as that in the tip clearance of 1.5 mm case. The tip clearance mainly affects the radial force change in the front section of the impeller in different cavitation cases. In essence, the tip clearance size has little impact on the radial force of the impeller.

Figure 11 shows the radial force in the impeller region.

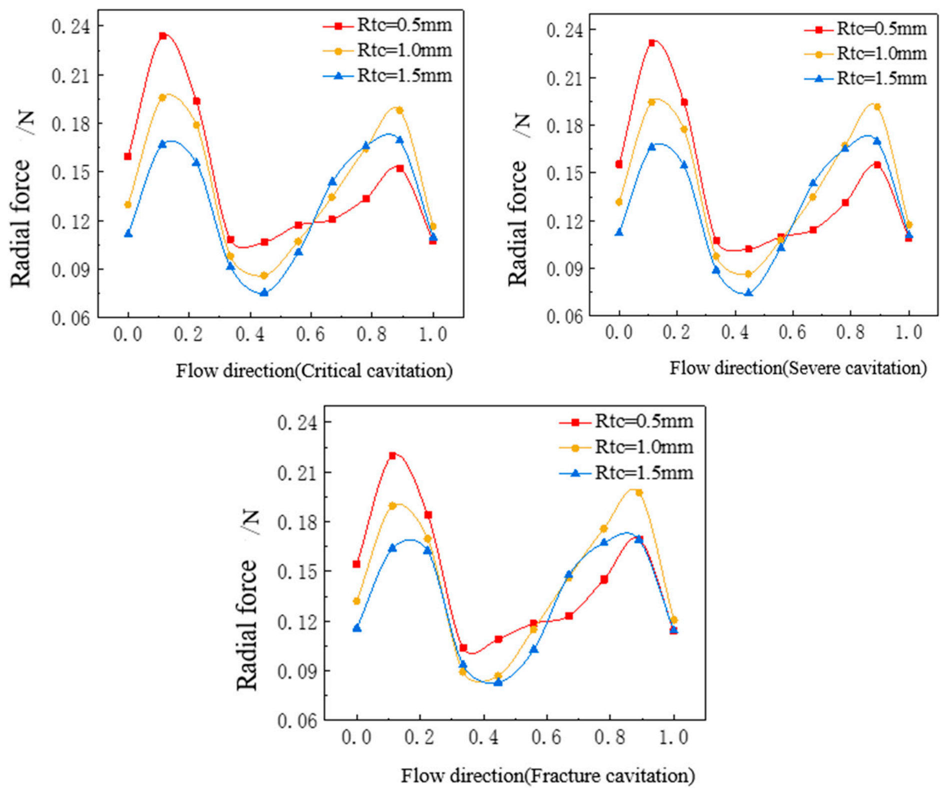

Figure 11. Radial force in the impeller of the SABP at different tip clearance sizes.

4.5. Effect of Tip Clearance on Axial and Radial Force of the Diffuser

Figure 12 shows the axial force in the diffuser.

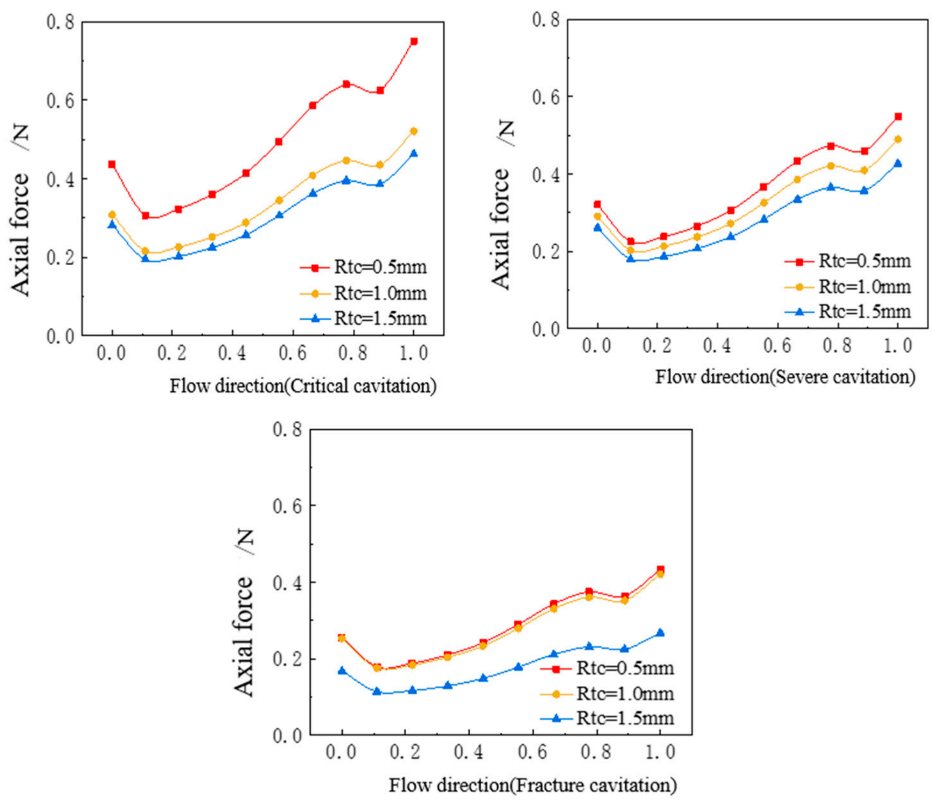

Figure 12. Axial force in the diffuser of the SABP at different tip clearance sizes.

From Figure 12, the regulation of axial force from the diffuser inlet to the outlet is the same in different cavitation cases. In the critical cavitation case, the tip clearance impacts the axial force on the rear section of the diffuser. Under each clearance condition, the axial force gradually declines along the flow direction from 0 to 0.1, and gradually increases along the flow direction from 0.1 to 1.0. The axial force reduces in the flow section of the diffuser with the growth of the tip clearance. In the severe cavitation stage, the axial force at 0.5 mm tip clearance decreases significantly, but other changes are the same as in the critical cavitation case. In the fracture cavitation case, the axial force declines further with the intensification of cavitation. The axial force curves at tip clearance of 0.5 mm and 1.0 mm are very similar. In summary, with the intensification of cavitation, the axial force is least affected under the condition of 1.0 mm tip clearance.

Figure 13 displays the radial force in the diffuser. From Figure 13, the radial force changes from diffuser inlet to diffuser outlet in different cavitation stages are consistent. In the critical cavitation stage, the effect of tip clearance size on the radial force mainly concentrates in the front section of the flow direction, and the radial force reaches the maximum value at the 0.1 section of the flow direction under all clearance conditions, and reduces with the growth of tip clearance. In the severe cavitation stage, the influence of tip clearance on radial force shows the same variation law as that of critical cavitation. In the fracture cavitation stage, the effect of tip clearance size on radial force still shows no noticeable change, demonstrating the same changing law as the previous two cavitation stages.

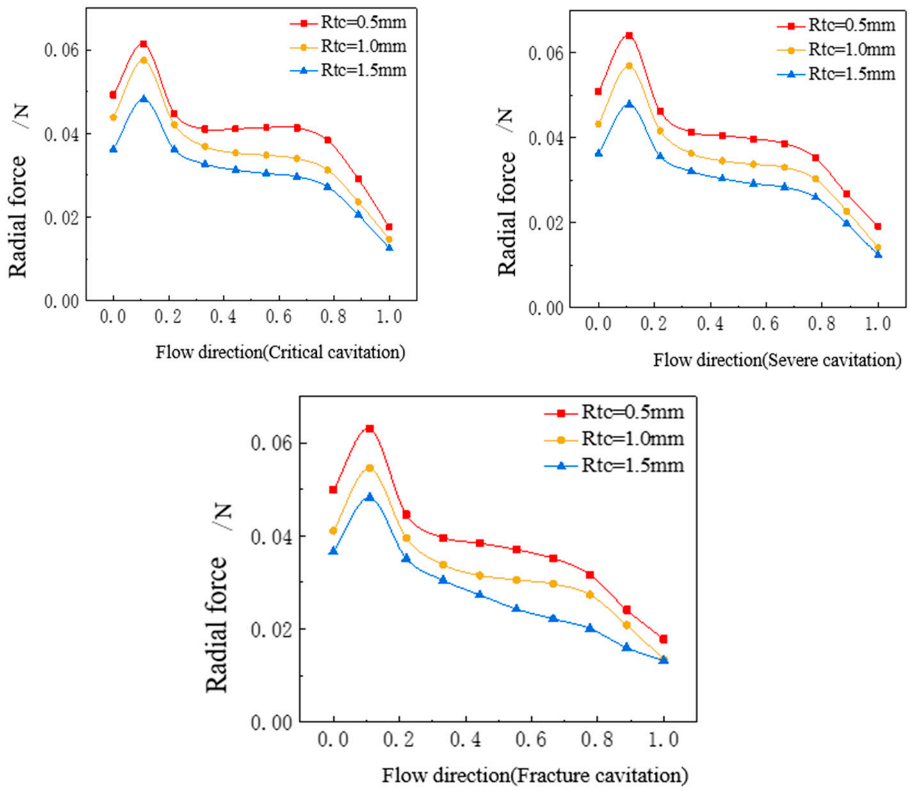

Figure 13. Radial force in the diffuser of the SABP at different tip clearance sizes.

5. Conclusions

The force characteristics of the SABP booster unit under different tip clearance sizes in different cavitation stages were analyzed in detail. Firstly, the pressure load under different tip clearance cases and different cavitation cases was analyzed; then, the effect of tip clearance size was observed through the changes in axial and radial force distribution. The main conclusions are as follows:

(1) From the pressure load under different tip clearance sizes and cavitation conditions, the diffuser inlet section and diffuser outlet section have sudden pressure changes

caused by dynamic and static interference. During the critical cavitation case, the pressure on the impeller blade PS reduces with the growth of tip clearance size, while the pressure on SS only reduces with the growth of tip clearance size at the first half of the impeller blade. The pressure on the flow section in the diffuser declines with the growth of tip clearance size. With the intensification of cavitation, it can be found that only at the tip clearance of 1.0 mm, is the influence the least, and the pressure curve drops the most slowly.

(2) From the distribution curves of axial and radial forces under different tip clearance sizes and cavitation conditions, the influence of axial force mainly concentrates on the back part of the impeller, and the influence of radial force mainly concentrates on the front part of the impeller. The axial and radial forces in the diffuser have a greater influence on the flow to the back section. The axial force declines with the growth of tip clearance size in the flow direction of the booster unit, while the radial force reduces with the increase in tip clearance size only in the diffuser region. With the increase in cavitation degree, it can be found that the axial force distribution is least affected at the tip clearance size of 1.0 mm.

Author Contributions: Conceptualization, H.W. and G.S.; methodology, H.W. and H.M.; software, L.L. and X.P.; writing—original draft preparation, H.W. and L.L.; writing—review and editing, H.W.; supervision, G.S. All authors have read and agreed to the published version of the manuscript.

Funding: This work was supported by the Open Research Subject of the Key Laboratory of Fluid and Power Machinery (Xihua University), Ministry of Education (Grant number LTDL-2023017).

Institutional Review Board Statement: Not applicable.

Informed Consent Statement: Not applicable.

Data Availability Statement: Data are contained within the article.

Conflicts of Interest: The authors declare no conflict of interest.

References

1. Meerakaviyad, D.; Keville, T.; Prakash, A.; Sajid, A.; Hamad, F. Recent progress in multiphase flow simulation through multiphase pumps. *Heat Transf.* **2020**, *49*, 2849–2867. [CrossRef]
2. Hu, H.; Li, X.K.; Gu, B. Hydraulic optimization of multiphase pump based on CFD and genetic algorithm. *Int. J. Grid Distrib. Comput.* **2015**, *8*, 161–170.
3. Kim, J.H.; Lee, H.C.; Kim, J.H.; Choi, Y.S.; Yoon, J.Y.; Yoo, I.S.; Choi, W.C. Improvement of hydrodynamic performance of a multiphase pump using design of experiment techniques. *J. Fluids Eng.* **2015**, *137*, 081301. [CrossRef]
4. Yang, X.; Hu, C.; Hu, Y.; Qu, Z. Theoretical and experimental study of a synchronal rotary multiphase pump at very high inlet gas volume fractions. *Appl. Therm. Eng.* **2017**, *110*, 710–719. [CrossRef]
5. Yang, X.; Qu, Z.; Wu, Y. Frictional loss studies and experimental performance of a new synchronal rotary multiphase pump. *J. Fluids Eng.* **2011**, *133*, 041303. [CrossRef]
6. Liu, M.; Tan, L.; Cao, S. Influence of viscosity on energy performance and flow field of a multiphase pump. *Renew. Energy* **2020**, *162*, 1151–1160. [CrossRef]
7. Liu, M.; Tan, L.; Xu, Y.; Cao, S. Optimization design method of multi-stage multiphase pump based on Oseen vortex. *J. Pet. Sci. Eng.* **2020**, *184*, 106532. [CrossRef]
8. Shen, X.; Zhang, D.; Xu, B.; Ye, C.; Shi, W. Experimental and numerical investigation of tip leakage vortex cavitation in an axial flow pump under design and off-design conditions. *Proc. Inst. Mech. Eng. Part A J. Power Energy* **2021**, *235*, 70–80. [CrossRef]
9. Shen, X.; Zhang, D.; Liu, A.; Jin, Y.; Chen, J.; Shi, W. Cavitation characteristics of tip leakage vortex and suction side-perpendicular vortices in axial flow pump. *Trans. Chin. Soc. Agric. Eng.* **2018**, *34*, 87–94.
10. Zhao, W.; Cheng, C.; Xue, Z. Study on influence of tip clearance on external characteristics and cavitation performance of axial flow pump. *J. Lanzhou Univ. Technol.* **2022**, *48*, 56–64.
11. Zhang, H.; Zuo, F.; Zhang, D.; Shi, W. Formation and Evolution Mechanism of Tip Leakage Vortex in Axial Flow Pump and Vortex Cavitation Analysis. *Trans. Chin. Soc. Agric. Mach.* **2021**, *52*, 157–167.
12. Zhang, D.; Shi, L.; Cheng, J.; Pan, Q.; Shi, W. Experimental analysis of cavitation characteristics in impeller tip region of axial flow pump. *J. Zhejiang Univ. (Eng. Sci.)* **2016**, *50*, 1585–1592.
13. Zhang, D.; Wu, S.; Shi, W.; Pan, D.; Yao, J.; Zhang, G. Application and experiment of different turbulence models for simulating tip leakage vortex in axial flow pump. *Trans. Chin. Soc. Agric. Eng.* **2013**, *29*, 46–53.

14. Li, Y.; He, H.; Zhang, F. Effect of tip clearance on cavitation flow in impeller of inclined flow pump. *J. Drain. Irrig. Mach. Eng.* **2020**, *38*, 224–229. (In Chinese)
15. Li, Y.; Hu, P.; Li, R. Numerical analysis of the effect of different tip clearance on the performance of inclined flow pump. *Trans. Chin. Soc. Agric. Eng.* **2014**, *30*, 86–93. (In Chinese)
16. Han, J.; Li, P.; Zhong, J. Effect of tip clearance on cavitation performance of water-jet propulsion axial-flow pump. *Sci. Technol. Eng.* **2016**, *16*, 130–136.
17. Shi, W.; Li, T.; Zhang, D. Influence of different tip clearance on cavitation performance and flow field of axial flow pump. *J. Huazhong Univ. Sci. Technol. (Nat. Sci. Ed.)* **2013**, *41*, 21–25. (In Chinese)
18. Zhang, H.; Zuo, F.; Zhang, D. Evolution mechanism of tip leakage vortex formation and vortex cavitation analysis in axial flow pump. *Trans. Chin. Soc. Agric. Mach.* **2021**, *52*, 157–167. (In Chinese)
19. Han, C.; Xu, S.; Cheng, H.; Ji, B.; Zhang, Z. LES method of the tip clearance vortex cavitation in a propelling pump with special emphasis on the cavitation-vortex interaction. *J. Hydrodyn.* **2020**, *32*, 1212–1216. [CrossRef]
20. Xu, M.; Cheng, H.; Ji, B.; Peng, X. LES of tip-leakage cavitating flow with special emphasis on different tip clearance sizes by a new Euler-Lagrangian cavitation model. *Ocean. Eng.* **2020**, *213*, 107661. [CrossRef]
21. Shamsuddeen, M.M.; Park, J.; Choi, Y.S.; Kim, J.H. Unsteady multi-phase cavitation analysis on the effect of anti-cavity fin installed on a Kaplan turbine runner. *Renew. Energy* **2020**, *162*, 861–876. [CrossRef]
22. Xu, B.; Shen, X.; Zhang, D.; Zhang, W. Experimental and numerical investigation on the tip leakage vortex cavitation in an axial flow pump with different tip clearances. *Processes* **2019**, *7*, 935. [CrossRef]
23. Fanning, D.T.; Gorrell, S.E.; Maynes, D.; Oliphant, K. Contributions of tip leakage and inlet diffusion on inducer backflow. *J. Fluids Eng.* **2019**, *141*, 121102. [CrossRef]